

Journal of Molecular Structure (Theochem) 496 (2000) 163-173



www.elsevier.nl/locate/theochem

Density functional study of structural and electronic properties of silane adsorbed Si(100) surface

J.S. Lin^{a,*}, Y.T. Kuo^a, M.-H. Lee^b, K.-H. Lee^b, J.C. Chen^a

^aDepartment of Chemistry, Tamkang University, Tamsui 25137, Taiwan, ROC ^bDepartment of Physics, Tamkang University, Tamsui 25137, Taiwan, ROC

Received 5 December 1998; received in revised form 17 May 1999; accepted 17 May 1999

Abstract

Ab initio total energy calculations based on a norm-conserving optimized pseudopotential and density functional theory with a generalized gradient approximation (GGA) have been used to study the structures and energetics in connection with Si(100) surface and the silane (SiH₄) adsorbed Si(100) surface. The electronic properties, i.e. layer-resolved density of state and atomic-resolved density of state, of Si(100)-(2 \times 2) surface and Si(100)-(2 \times 2) (SiH₃:H) surface have been calculated. The surface electronic states arising from the buckled Si=Si dimer are characterized to illustrate the bonding nature of Si(100)-(2 \times 2) and Si(100)-(2 \times 2) (SiH₃:H). © 2000 Elsevier Science B.V. All rights reserved.

Keywords: Density functional theory; Pseudopotential; Chemical vapor deposition; Silane; Si(100) surface; Density of state

1. Introduction

Silicon thin film is routinely grown from gaseous molecules in a variety of chemical vapor deposition (CVD) processes, and silane (SiH₄) is the most common CVD precursor for Si, SiO₂ and other materials. During the CVD growth of Si film, SiH₄ initially adsorbs onto the surface of the growing film and then the decomposition of surface SiH_x (x = 1, 2, 3) leads to film growth and H₂ as a byproduct.

Despite the fact that CVD of SiH₄ on the Si(100) surface has been investigated [1–3] thoroughly with a temperature programmed desorption technique and a static secondary ion mass spectrometry, understanding of (1) both dissociation and formation of covalent bonds as SiH₄ adsorbs, (2) surface SiH_x fragments decomposition, and (3) Si film growth still remain

It has been suggested [1] that during the dissociative adsorption of SiH₄ onto Si(100) surface, SiH₃ and H are the initial products and dangling bonds are required for the initial dissociative adsorption step. Therefore, the stability of SiH₃ adsorbed Si(100) surface depends on the local environment, i.e. coverage of dangling bond, near this species. In addition to providing adsorption sites, the dangling bonds serve as reactive sites for the decomposition of surface intermediates. As a result, the dangling bonds can also act in a way to control the competition of parallel reaction paths on that surface.

In a recent paper [4], Kruger and Pollmann

extremely difficult. Moreover, the electronic properties of Si(100) surface have a significant influence on the way SiH₄ molecule adsorbs on this surface. Therefore, it is of a paramount importance to investigate the nature of the surface electronic states arising from Si(100) surface and their roles during the dissociative adsorption of SiH₄ onto this surface.

^{*} Corresponding author. Fax: + 886-2-2622-8458. *E-mail address:* jsl@mail.tku.edu.tw (J.S. Lin).

suggested that the buckled Si=Si dimer on the Si(100) surface, i.e. Si(100)-(2 × 2), after reconstruction is more stable than the symmetrical Si=Si dimer, i.e. Si(100)- (2×1) , on the same surface. They also proposed that for Si(100) surface, the π interaction would cause the formation of symmetrical Si=Si dimer and it would lead to a metallic state. However, in this case, the Jahn-Teller-like distortion leads to buckled Si=Si dimers. As a result, the Si=Si dimer on the Si(100) surface is semiconducting. To rationalize further this interesting feature, they proposed that this Jahn-Teller-like distortion could be traced back to electronic properties of the constitutent atoms. For example, the 2p orbitals of C are more localized than the 2s orbitals since there are no p states in the C core. Therefore, p-like orbitals of C are able to localize their charges in the bonding region, which leads efficiently to a strong tendency of π bond formation [5]. However, for Si, the tendency of forming a π bond is clearly suppressed, since in this material the p valence orbitals are more extended than the s valence ones. Therefore, the charges of p-like orbitals of Si are energetically favorable to polarization through the Jahn-Teller-like distortion, thereby weakening the Si=Si bond strength. Apparently, this formation of buckled Si=Si dimer with the dangling bonds on the Si(100) surface is crucial for rationalizing the mechanism of SiH₄ dissociative adsorption onto the Si(100) surface [6,7].

Another recent work [8], that of Liu and Hoffmann, concerning about the acetylene chemisorbed Si(100) surface suggested that there is partial electron transfer to the buckled-up Si, making it a nucleophilic site. The buckled-down Si atom should be electrophilic. In other words, the buckling of Si=Si dimer has substantial effects on the electronic structure and the chemical reactivity of the Si(100) surface. Therefore, we believe that the surface electronic states arising from the buckled Si=Si dimer play a key role in understanding of its reactivity toward silane. In addition, more recent work of Konecny and Doren [9] and Fattal et al. [10] which explore the H₂O and BH₃ adsorption on Si(100)-(2 \times 1) and NH₃ adsorption on Si(100)-(2 × 1), respectively, suggest that the buckling of Si=Si dimer affects the overlap of the surface orbitals with the reactants. Furthermore, Konecny and Doren introduce the concept of mixing π and π^* orbitals, increasing the HOMO-LUMO splitting and introducing a Si–Si anti-bonding component into the HOMO to intepret the correlation of surface orbitals with their reactivities. Finally, they use the calculated Mulliken charges to illustrate an asymmetric surface electron distribution. They state that many features of the reaction path and adsorbate geometry can be rationalized in terms of the difference in electron density at the two sites.

Although many theoretical studies of surface chemistry on Si surfaces based on cluster models [8-15] have been reported recently, the study of forming and breaking of covalent bonds as SiH4 adsorbs on different Si surfaces is still extremely difficult. In addition, for the finite sizes of cluster model, it is unlikely to include a long-range interaction through the whole Si surface and to treat the edge effect precisely. Recently, Penev et al. [16] investigated the effect of the cluster size in modeling the H2 desorption and dissociative adsorption on Si(100), and suggested that the smaller clusters generally overestimate the activation barrier and reaction energy. They even suggested that some of the previous works using smaller clusters will need revision. In this study, we therefore devote ourselves to the density functional study of the energetic, structural and electronic properties of buckled Si=Si dimer, i.e. Si(100)-(2 \times 2), and SiH₄ adsorbed Si(100)-(2 \times 2) surface, i.e. Si(100)-(2 \times 2) (SiH₃:H), using periodic slab model. We also calculated the layer-resolved density of states (LDOS) [17,18] and atomic-resolved density of states (ADOS) [17,18], to illustrate the electronic properties of Si(100)-(2 \times 2) surface and their effects on the energetics of dissociative adsorption of SiH₄ onto this surface. In particular, we introduced the ADOS to investigate the bonding nature of Si(100)-(2 \times 2), and clearly explain how Jahn-Teller-like distortion influences the chemical reactivity in connection with SiH₄ dissociative adsorption onto this surface.

2. Computational methods

Density functional theory (DFT) [19] with a generalized gradient approximation (GGA) is applied to perform the ab initio total energy pseudopotential calculations [20,21]. This technique allows one to calculate the relative energies of chosen atomic configurations and has been shown to yield an

Table 1 The energy cut-off tests for the bond length of Si-H within SiH₄ and the dissociative adsorption energy of SiH₄ adsorbed onto the Si(100)-(2 \times 2) surface

Energy cut-off (eV)	Si-H bond length (Å)	E _{ads.} (eV)	
200	1.514	1.984	
300	1.493	1.966	
400	1.487	1.958	
500	1.484		
600	1.481		
Experimental	1.4798		

extremely high degree of accuracy. Our computational strategy is to perform all the calculations using periodic boundary condition (sometimes known as the supercell method), with the electronic orbitals represented by using a plane-wave basis set. We have used an ab initio molecular dynamic method based on the conjugated gradient technique [22] to minimize the Kohn-Sham energy functional in which the GGA of Perdew and Wang [23] is utilized. For the brillouin-zone integration, we used a $2 \times 2 \times 1$ grid of Monkhorst-Pack special points after a convergence test of structural and energetic data of Si(100) with a grid of $3 \times 3 \times 1$ [24]. We also explored the plane-wave convergence tests by calculating the structural parameter of SiH₄, i.e. bond length of Si-H, and dissociative adsorption energy of SiH₄ adsorbed onto the Si(100) surface as reported in Table 1. Our calculated bond length of Si-H with a cut-off of 300 eV is 0.006 Å larger than that of 400 eV and our calculated dissociative adsorption energy of SiH₄ adsorbed onto Si(100) with a cut-off of 300 eV is only 0.008 eV larger than that of 400 eV. These results clearly indicate that the energy cut-off of 300 eV is enough for the calculated physical and chemical properties of our interest. A Kleinman-Bylander representation [25] of the pseudopotential is used. This allows the plane-wave matrix elements of the pseudopotential to be expressed in a separable form for computational efficiency. In our calculations, the Si(100)-(2 \times 2) surface was represented by periodically repeated slabs of Si atoms, i.e. primitive 2×2 unit cell (six layers in the unreconstructed geometry) with one side of three layers fixed and other side of three layers followed by a vacuum region of approximately 13 Å. These vacuum layers are mainly introduced to avoid the interaction between surfaces due to

the periodicity along the [100] direction. Finally, our choice of unit cell size can only apply to a higher coverage of SiH_4 adsorbed onto the Si(100) surface.

The pseudopotential of silicon was constructed as usual from an all-electron atomic calculation, with the condition of norm conservation [26-28] and the continuity of the pseudo-wavefunction and its first and second derivatives at the core radius. We have used the standard Kerker method of pseduopotential generation [29], with a reference atomic configuration of $3s^23p^2$ for s and p components and $3s^23p^{\bar{0}.75}3d^{0.25}$ for the d component, and core radii of 1.80 a.u. The swave component was taken to be the local for the Kleinman-Bylander representation. The pseudopotential generation of oxygen requires great care because the valence 2p orbitals do not have core states. Consequently, the p-wave pseudopotential is strongly attractive and enormous number of planewave is needed to represent the valence pseudo-wavefunction. This type of pseudopotential has one additional requirement to those mentioned above, namely, that the kinetic energy associated with each pseudowavefunction has to be minimized. Therefore, we have used the method [30-32] of optimized pseudopotential generation, with a reference atomic configuration of $2s^22p^4$ for s and p components and $2s^22p^{2.5}3d^{0.5}$ for the d component, with the core radius for these three components taken as 1.25, 1.25 and 1.45 a.u. In this case, the s-wave component has been treated as local. Although both O and Si pseudopotentials are constructed using only the local density approximation (LDA), they have been shown to be highly transferable over the required energy ranges from neutral atoms, positive ions [30-32], silicon surface reconstruction [33] and MgO properties [34]. A pure Coulomb potential is used for hydrogen throughout this study.

To obtain the LDOS and ADOS, we generated the total density of state (TDOS) of whole system using a reasonable number of K-points and bands (normally a few more than occupied bands). Then, we decomposed the TDOS into the contribution of occupied bands of partial fragments, i.e. one layer, of the whole system to give rise to LDOS. Finally, we decomposed further the LDOS into the contribution of occupied bands of atomic components, i.e. one atom, to generate the ADOS. Here, we have to introduce the space cut for each atomic component of partial fragment to exclude the unnecessary contribution from other neighboring

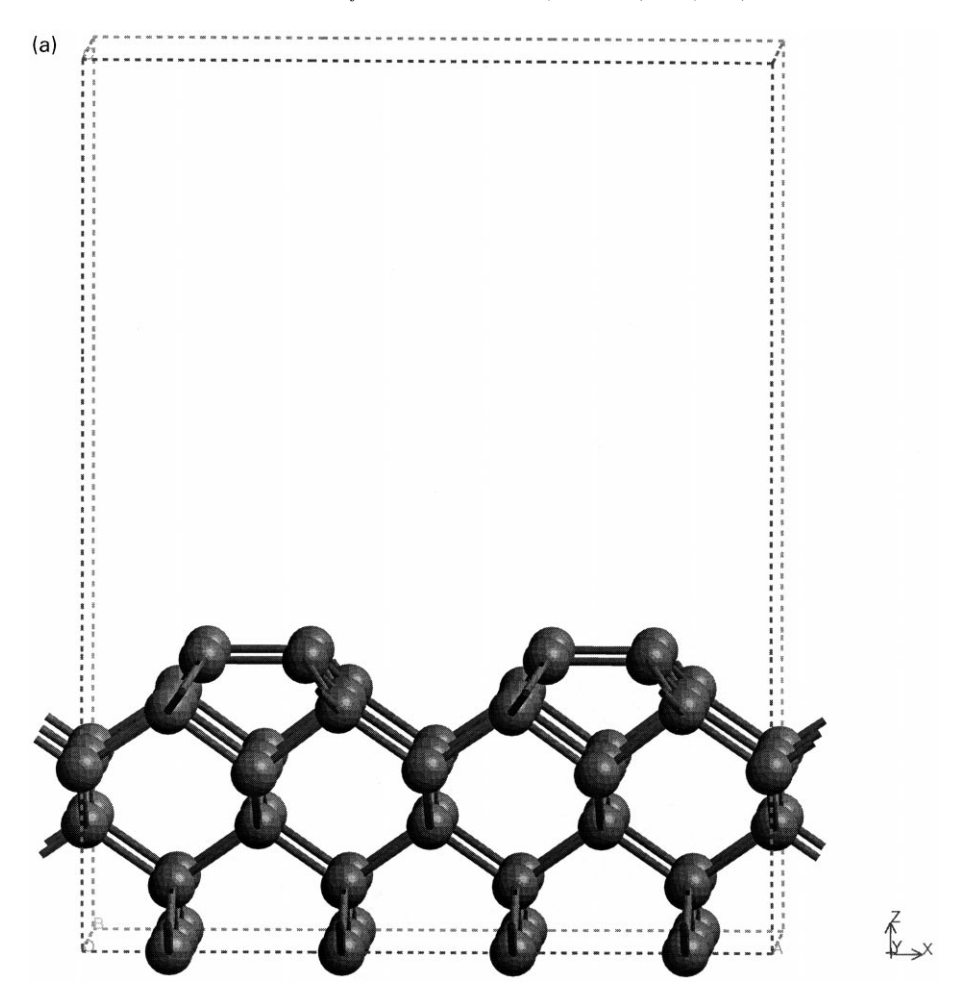


Fig. 1. The side view of (a) the relaxed symmetrical Si=Si dimer and (b) the relaxed buckled Si=Si dimer on the Si(100) - (2 × 2) surface. Unit cell model is shown twice.

atoms. In this study, we only consider Si as the constituent atom of partial fragments to generate the LDOS and ADOS, and its space cut is chosen to be half of Si–Si bond length of bulk silicon. We performed all the total energy, LDOS and ADOS calculations using the modified version of CASTEP 3.5 [39].

3. Calculated results and discussion

3.1. Surface structure of Si(100)- (2×2)

As an initial step in this study, we have investigated the surface structure of buckled Si=Si dimer, i.e. Si(100)-(2 × 2). The calculated relaxed structure is shown in Fig. 1 and the calculated relevant structural parameters after relaxation are reported in Table 2. Our calculated structural model, with a buckled Si=Si dimer bond length $d_{11}=2.31\,\text{Å}$ which is $0.02\sim0.04\,\text{Å}$ larger than that of a recent work of Doren [11,12] using a Si₉H₁₂ cluster to model the reconstructed Si(100)-(2 × 1) surface, predict the buckling angle 9.7° which is about 1.0° larger than that of the above work [11,12]. Also, both calculated and buckled Si=Si dimer bond lengths are slightly smaller than the bond length (2.33 Å) of Si–Si single bond in the Si₂H₆ molecule. Subsequently, there may be some π bonding characters in the buckled Si=Si

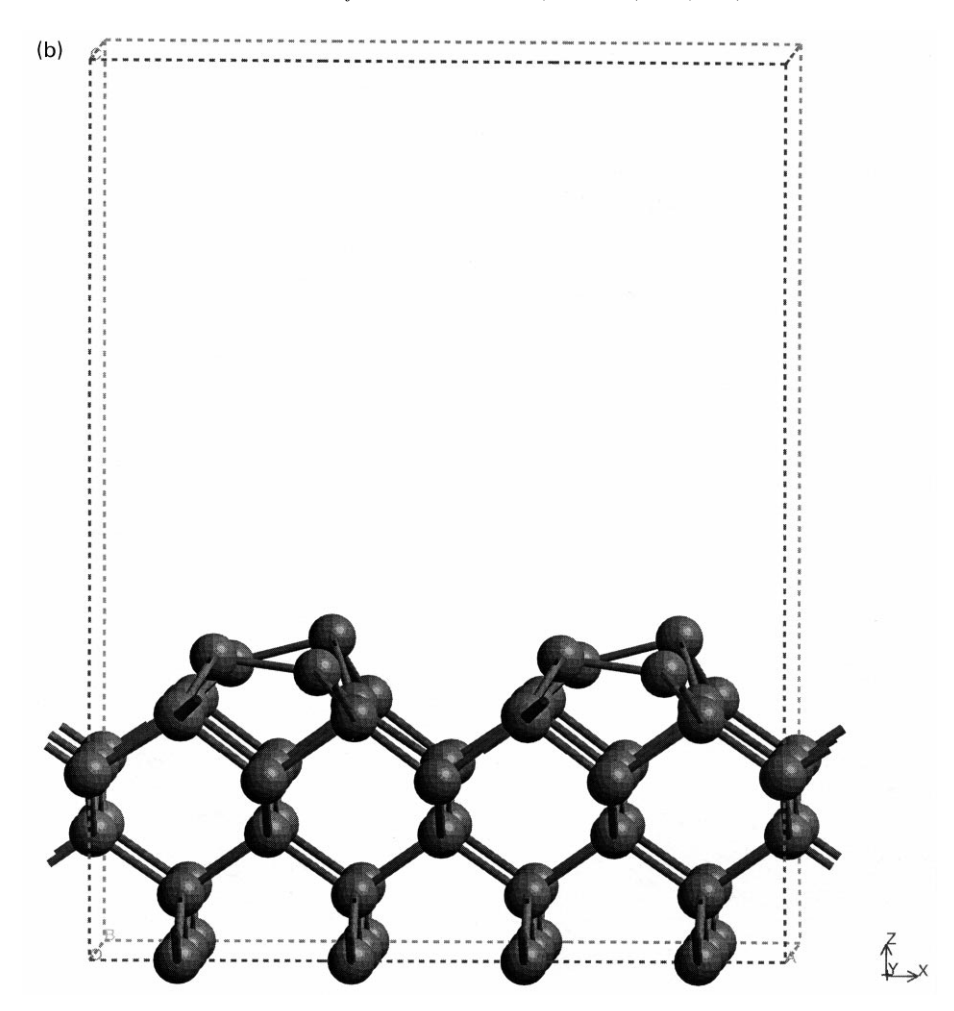


Fig. 1. (continued)

dimer. In addition, the reconstruction of Si(100) surface also leads to a slight contraction of the Si–Si distance between the first and second layer to $d_{12}=2.33$ Å. These calculated structural parameters are shown to be consistent with other theoretical works [35,36]. To explore this buckled Si=Si dimer in more detail, we present the contour of total valence charge density as shown in Fig. 2. This contour clearly shows unevenly distributed valence charge density in the buckled Si=Si dimer bond region. This is in agreement with the Hoffmann's and Doren's group view of the buckled-up atom as a nucleophilic site and buckled-down atom as an electrophilic site. We also believe that this unevenly distributed valence charge

density is one of the main factors controlling the initial products of SiH₄ dissociative adsorption onto the Si(100) surface which will be discussed in later sections.

3.2. Electronic property of Si(100)- (2×2)

As mentioned earlier, the dangling bonds on the Si(100) surface are required for the initial step of SiH_4 dissociative adsorption onto this surface. Therefore, it is important to have a better view into the electronic properties of Si(100)-(2 × 2) surface in order to rationalize the effect of these dangling bonds on the SiH_4 adsorption reaction mechanism.

Table 2 The calculated bond lengths (Å) in the relaxed symmetrical Si=Si dimer on Si(100), i.e. Si(100)-(2 × 2), and the relaxed buckled Si=Si dimer on Si(100), i.e. Si(100)-(2 × 2). The d_{12} is the distance between the top layer of Si, i.e. the Si=Si dimer, and second layer of Si. The d_{23} is the distance between the second layer and third layer. The d_{34} is the distance between the third layer and fourth layer

	Relaxed buckled Si=Si dimer	Relaxed symmetrical Si=Si dimer
Si=Si dimer (1) (Å)	2.315	2.301
Si=Si dimer (2) (Å)	2.354	2.301
d ₁₂ (Si–Si) (Å)	2.330	2.288
d ₂₃ (Si–Si) (Å)	2.383	2.344
d ₃₄ (Si–Si) (Å)	2.389	2.361

To elaborate this, we consider now the calculated LDOS of Si(100)- (2×2) surface. The first layer of the upper three layers of Si(100)- (2×2) slab, i.e. the buckled Si=Si dimer, is used to represent the fully relaxed Si(100)- (2×2) surface. Our calculated results for the LDOS of bulk Si and fully relaxed Si(100)- (2×2) surface are presented in Fig. 3. Compared to the bulk Si, the fully relaxed Si(100)- (2×2) surface shows occupied surface states within an interval of about 0.5 eV from the fermi level. These occupied surface states are mainly characteristic of the dangling bonds involving a π bond for the Si=Si dimer formation. As for the occupied surface states within an interval of about 1.2 eV from the fermi level, they are mainly characteristic of the dangling bonds directly

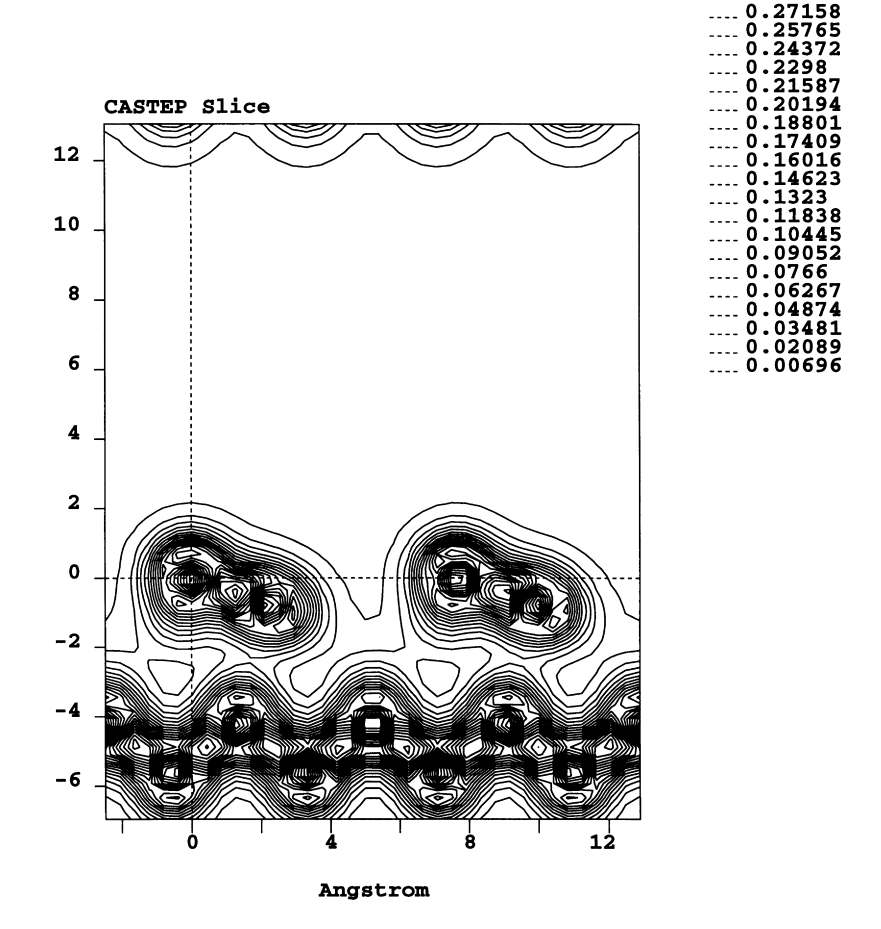


Fig. 2. The contours of the total valence charge density for the buckled Si=Si dimer through the cut along the Si=Si dimer. Contour lines are drawn at intervals of 0.014 e Å^{-3} .

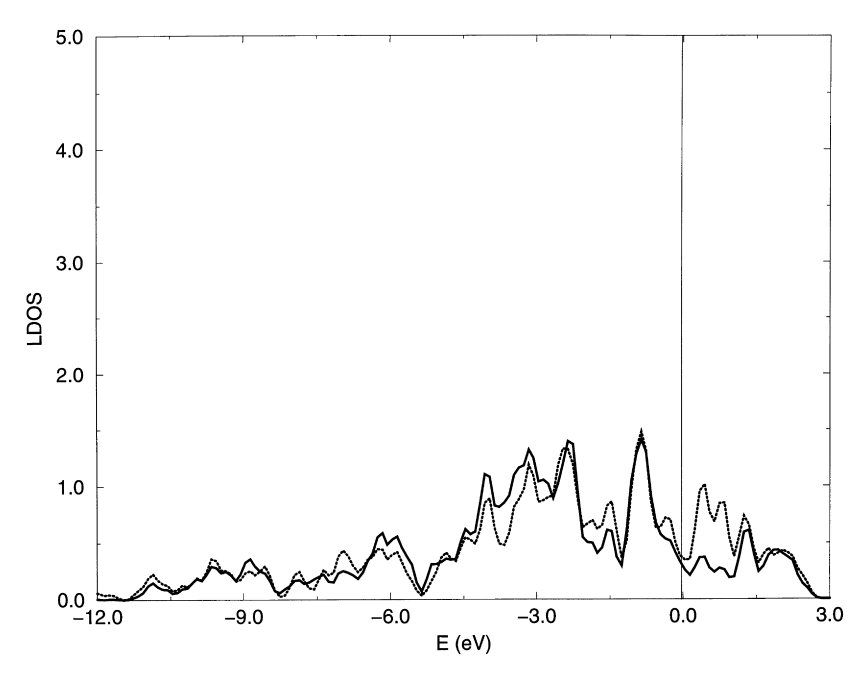


Fig. 3. The layer-resolved density of states (LDOS) of bulk Si, i.e the fourth layer, (full line) and the relaxed Si(100)- (2×2) surface, i.e. the first layer, (dotted line). The vertical line at zero indicates the fermi level.

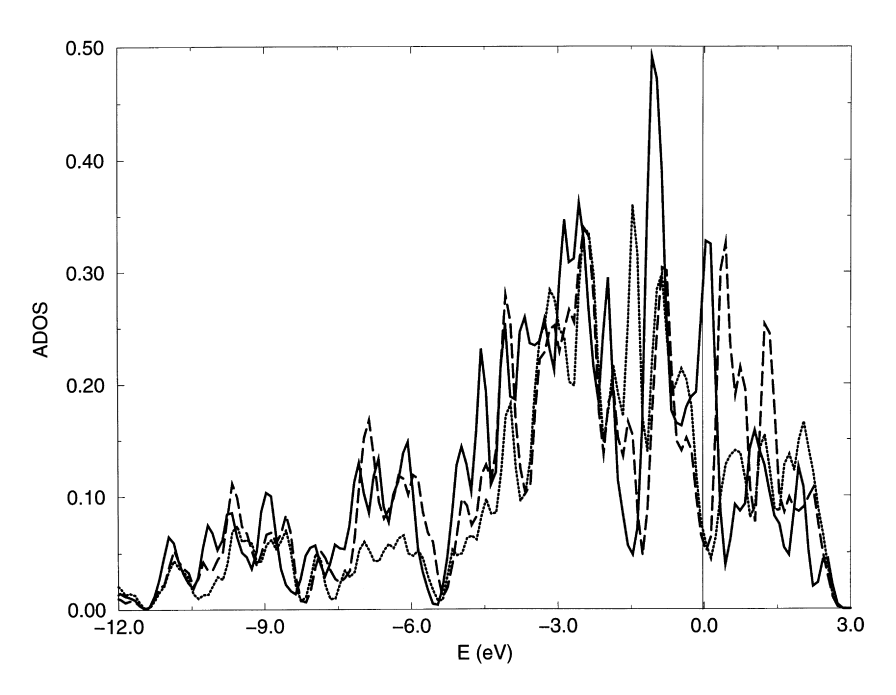


Fig. 4. The atom-resolved density of states (ADOS) of Si atom on the symmetrical Si=Si dimer (full line), the buckled-up Si atom on the buckled Si=Si dimer (dotted line) and the buckled-down Si atom on the buckled Si=Si dimer (dashed line).

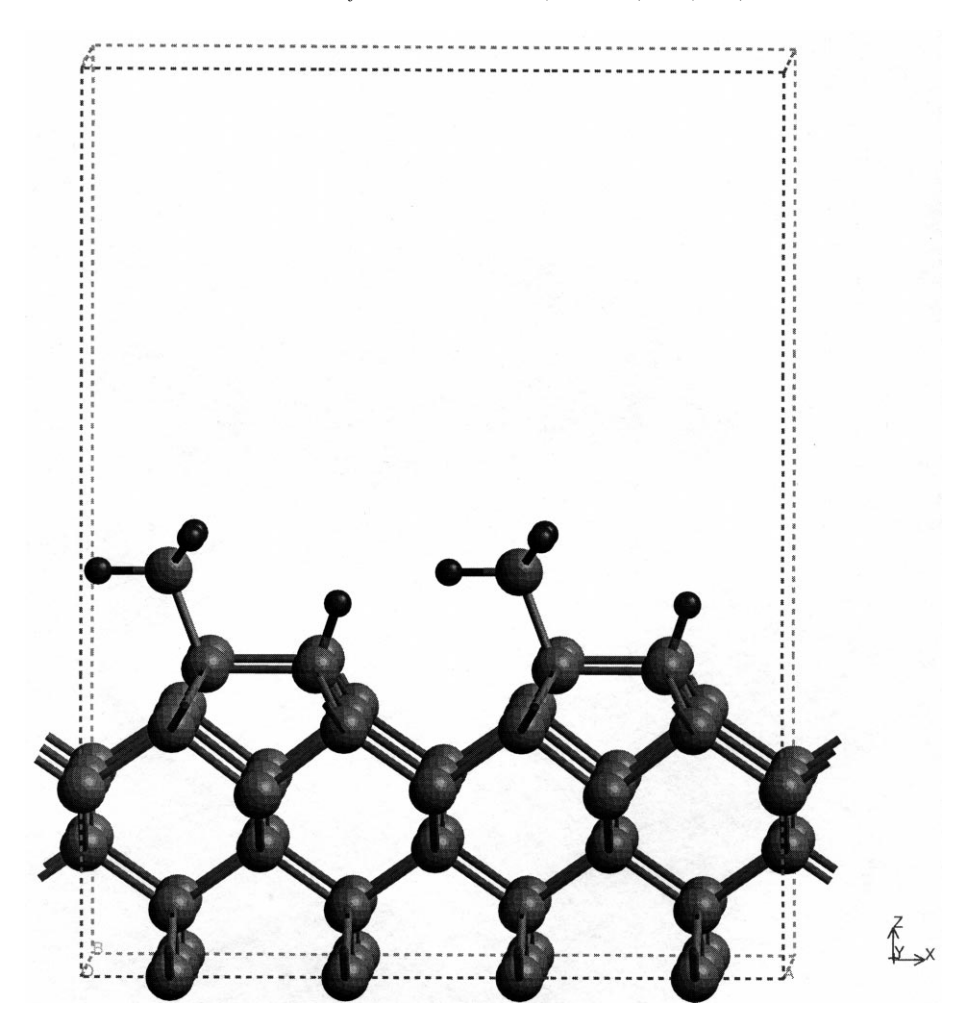


Fig. 5. The side view of SiH₄ adsorbed Si(100)-(2 \times 2) i.e. Si(100)-(2 \times 2) (SiH₃:H).

involving a σ bond within the Si=Si dimer. Finally, there are empty surface states within the gap.

Then, we calculated the ADOS of buckled and symmetrical Si=Si dimer on the Si(100) surface in order to rationalize, from an electronic state point of view, the symmetrical-to-buckled relaxation at the Si(100) surface due to the Jahn-Teller effect in molecules with a symmetry-degenerated ground state. By ADOS, we mean that the DOS of only one Si atom on Si=Si dimers is calculated. Since the dangling bonds of Si=Si dimer are predominantly of p-character, the calculated ADOS contains only the contribution of p-component of Si atoms. We compared the ADOS of buckled-up Si atom with that of Si atom on the

symmetrical Si=Si dimer as shown in Fig. 4. Indeed, the formation of the symmetrical Si=Si dimer on the Si(100) surface will cause disappearance of the band gap around the fermi level. In addition, our calculated ADOS of the symmetrical Si=Si dimer which appears as a single peak around the fermi level will split into two peaks when a Jahn-Teller-like distortion occurs, i.e. becomes a buckled Si=Si dimer. This result is consistent with the breaking of the molecular symmetry thereby causing the formation of non-degenerated electronic states. We also considered the energy needed to allow the change between the symmetrical dimer and the buckled dimer. Our calculated energy of 0.09 eV is so small that two possible buckled

Table 3 The calculated bond lengths (Å) and the bond angles (°) of SiH₄ above the Si(100)-(2 × 2) surface (Sa), the SiH₄ adsorbed Si(100)-(2 × 2) surface (Sb), i.e. Si(100)-(2 × 2) (SiH₃:H), and the corresponding dissociative adsorption energy E_{ads} , which is calculated approximately as E(Sa) - E(Sb). The zero in the parentheses after Si indicates Si within SiH₃ or SiH₄ and one in the parentheses after Si indicate the Si atom on the relaxed buckled Si=Si dimer of Si(100)-(2 × 2) (SiH₃:H)

	SiH_4 above $Si(100)$ - (2×2)	SiH_4 adsorbed $Si(100)$ - (2×2)	
Si=Si dimer (1) (Å)	2.313	2.385	
Si=Si dimer (2) (Å)	2.355	2.289	
d_{12} (Si–Si) (Å)	2.329	2.349	
d ₂₃ (Si–Si) (Å)	2.382	2.352	
d ₃₄ (Si–Si) (Å)	2.393	2.375	
∠H Si(0) H (°)	109.5	110.7	
$\angle Si(0)Si(1)Si(1)$ (°)		110.4	
∠H Si(1)Si(1) (°)		109.8	
$E_{\rm ads.}$ (eV)		1.966	

orientations will rapidly flick at ambient temperature. Finally, when compared to the calculated ADOS of buckled-up Si atom with that of buckled-down Si atom, we found that the ADOS peak (~ -0.5 and ~ -1.5 eV) associated with non-degenerate electronic states of buckled-up Si atom have higher density than that of buckled-down Si atom. These calculated results also support both Hoffmann's and Doren's statements [8,11] that there is slightly higher electron density around the buckled-up Si atom than that around the buckled-down Si atom on the buckled Si=Si dimer of the Si(100)-(2 \times 2) surface.

3.3. Geometrical structure of Si(100)- (2×2) (SiH_3 :H)

It has been suggested [1] that during the dissociative adsorption of SiH₄ onto the Si(100) surface, both SiH₃ and H are the initial products, and dangling bonds are required for the initial dissociative adsorption step. A detailed mechanism of the dissociative adsorption of SiH₄ onto the Si(100) surface have been discussed elsewhere [12,37]. Here, we emphasize qualitatively the influence of electronic properties of the Si(100)-(2 \times 2) surface on the reaction path of SiH₄ dissociative adsorption onto this surface. To demonstrate this, firstly we realized that our calculated relaxed surface model of Si(100)- (2×2) has only two buckled Si=Si dimers in parallel with each other within the unit cell as shown in Fig. 1. Therefore, we expect that the SiH₄ species will either adsorb on a buckled-up Si atom or on a buckled-down Si atom at least from the film growth point of view.

Secondly, due to the formation of buckled Si=Si dimers and the polarized electron pair toward H within the SiH₄ molecule, we reasonably assumed that SiH₄ molecules will probably form the bond to the buckled-up Si atom (nucleophilic site) on the buckled Si=Si dimer through SiH₃ within SiH₄, and then the H which is nearer to the buckled-down Si atom will dissociate and form a bond to the buckled-down Si atom (electrophilic site) on the buckled Si=Si dimer. Consequently, two new bonds are formed to the H and SiH₃ fragments from the two dangling bonds on Si atoms of the buckled Si=Si dimer. The final calculated structure of SiH4 adsorbed the Si(100)-(2 \times 2) surface, i.e. Si(100)-(2 \times 2) (SiH₃:H), is shown in Fig. 5. The corresponding energetic data, i.e. dissociative adsorption energy and structural parameters are presented in Table 3. To validate this calculated energetic data using DFT-GGA plus pseudopotential, we also calculated the bond strength of SiH₃-H. Our calculated bond strength of SiH₃-H gives 3.89 eV which is in good agreement with the experiment data (3.91 eV) of Walsh [38]. Of course, this qualitative description of dissociative adsorption of SiH₄ onto the Si(100) surface is not the only reaction path to form the Si(100)-(2 × 2) (SiH₃:H). For example, the SiH₄ could probably orient in such a way that the H within SiH₄ could act as a hydrid to attack the buckled-down Si atom (electrophilic site), then the SiH₃ fragment will gradually dissociate from SiH₄ and diffuse to form a bond to the buckled-up Si atom. In consequence, the same two bonds are formed to the H

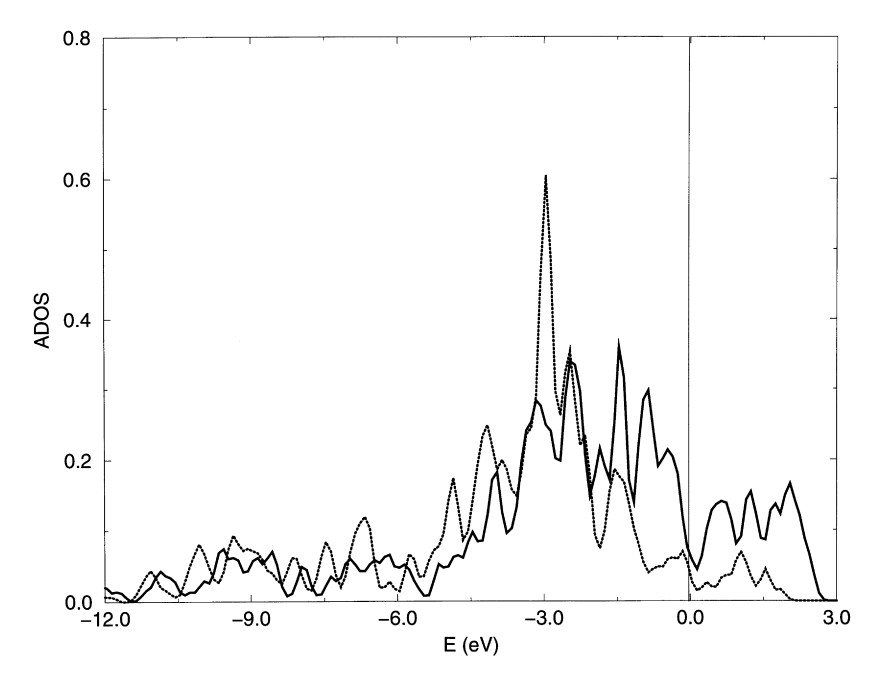


Fig. 6. The atom-resolved density of states (ADOS) of Si atom on the relaxed buckled Si=Si dimer of Si(100)-(2 \times 2) (full line) and ADOS of Si atom on the relaxed buckled Si=Si dimer of Si(100)-(2 \times 2) (SiH₃:H) (dotted line).

and SiH₃ fragments from the two dangling bonds on Si atoms of the buckled Si=Si dimer.

Our calculated results indicate that the dissociative adsorption of SiH₄ onto the Si(100)-(2 × 2) is energetically favorable and it leads to the stable structure of Si(100)-(2 × 2) (SiH₃:H). Our calculated dissociative adsorption energy (1.97 eV) is very similar to that of Doren [12]. Another factor worth to mention is that the bond length of the Si=Si dimer is elongated after the dissociative adsorption of SiH₄ onto the Si(100)-(2 × 2). This is due to the forming of sp³ hybrids of SiH₃-Si-Si-H from the original buckled Si=Si dimer. The cause of this elongation of Si=Si bond length will be discussed further in Section 3.4 using calculated ADOS.

3.4. Electronic property of Si(100)- (2×2) (SiH_3 :H)

We mentioned previously that the relaxed buckled Si=Si dimer of the Si(100)-(2 \times 2) surface provides the nucleophilic site on the buckled-up Si atom and the electrophilic site on the buckled-down Si atom. Therefore, during the process of the dissociative adsorption of SiH₄ onto the Si(100)-(2 \times 2) surface,

two new bonds are formed to the H and SiH3 fragments from the two dangling bonds on the dimerized Si=Si atoms. Consequently, we should expect that the bonding nature of the relaxed buckled Si=Si dimer of the Si(100)-(2 \times 2) surface will change to a certain extent to maintain the stability of the Si(100)- (2×2) (SiH₃:H) surface. To appreciate more about the bonding nature and the corresponding stability of the Si(100)-(2 × 2) (SiH₃:H) surface, the ADOS of Si atoms on the buckled Si=Si dimer and that on the relaxed buckled Si=Si dimer of the Si(100)-(2 \times 2) (SiH₃:H) surface are calculated. We compared the ADOS of Si atoms on the relaxed buckled Si=Si dimer of the Si(100)-(2 \times 2) surface with that of Si atoms on the relaxed buckled Si=Si dimer of the Si(100)-(2 × 2) (SiH₃:H) surface as shown in Fig. 6. The surface electronic states arising from the relaxed buckled Si=Si dimer within an interval of about 1.0 eV from the fermi level are diminished, and the empty surface states within the gap are reduced. Therefore, we believe that the Si atoms on the buckled Si=Si dimer of the Si(100)-(2 \times 2) (SiH₃:H) surface will behave more or less like the bulk Si atoms. Indeed, our calculated bond length of the Si=Si dimer, i.e. 2.39 Å, of Si(100)-(2 \times 2) (SiH₃:H) supports this statement.

4. Conclusion

Having combined slab model, density functional calculations (GGA), and corresponding analysis tools such as LDOS and ADOS, we are able to have a thorough study of the structure, energetics and bonding nature of the buckled Si=Si dimer on the Si(100) surface, i.e. Si(100)-(2 × 2), and the silane adsorbed $Si(100)-(2 \times 2)$ surface, i.e. $Si(100)-(2 \times 2)$ (SiH₃:H). Firstly, our calculated results suggest that the relaxation of Si(100) surface leading to the formation of the buckled Si=Si dimer, i.e. Si(100)-(2 \times 2), is crucial for understanding the dissociative adsorption of SiH₄ onto this surface. Secondly, our calculated electronic properties of the symmetrical and buckled Si=Si dimer on the Si(100) surface, i.e. LDOS and ADOS, clearly indicate that there is a Jahn-Taller-like distortion from the symmetrical dimer. Finally, our calculated electronic properties of Si(100)-(2 \times 2) (SiH₃:H) using ADOS, illustrate the presence of the bulk nature of the Si=Si dimer on Si(100)-(2 \times 2) (SiH₃:H).

Acknowledgements

The authors would like to thank the financial support from the National Science Council in Taiwan (Grant No. 86-2113-M-032-012 and 87-2113-M-032-005), the use of computational facilities from the National Center for High Performance Computing and Tamkang University in Taiwan. The authours also like to thank Dr. Hytha for carefully rewriting the manuscript.

References

- S.M. Gates, C.M. Greenlief, D.B. Beach, J. Chem. Phys. 93 (1990) 7493.
- [2] S.M. Gates, C.M. Greenlief, D.B. Beach, P.A. Holbert, J.Chem. Phys. 92 (1990) 3144.
- [3] S.M. Gates, S.K. Kulkarni, Appl. Phys. Lett. 58 (1991) 2963.
- [4] P. Kruger, J. Pollmann, Phys. Rev. Lett. 74 (1995) 1155.

- [5] J. Furthmuller, J. Hafner, G. Kresse, Europhys. Lett. 28 (1994) 659
- [6] R.J. Hamers, Y. Wang, Chem. Rev. 96 (1996) 1261.
- [7] H.N. Waltenburg, J.T. Yates Jr., Chem. Rev. 95 (1995) 1589.
- [8] O. Liu, R. Hoffmann, J. Am. Chem. Soc. 117 (1995) 4082.
- [9] R. Konecny, D.J. Doren, J. Chem. Phys. 106 (1997) 2426.
- [10] E. Fattal, M.R. Radeke, G. Reynolds, E.A. Carter, J. Phys. Chem. B 101 (1997) 8058.
- [11] A.R. Brown, D.J. Doren, J. Chem. Phys. 109 (1998) 2442.
- [12] A.R. Brown, D.J. Doren, J. Chem. Phys. 110 (1999) 2643.
- [13] P.C. Weakliem, E.A. Carter, J. Chem. Phys. 98 (1993) 737.
- [14] M.R. Radekr, E.A. Carter, Surface Sci. 355 (1996) L289.
- [15] C.J. Wu, E.A. Carter, Chem. Phys. Lett. 185 (1991) 172.
- [16] E. Penev, P. Kratzer, M. Scheffler, J. Chem. Phys. 110 (1999) 3986
- [17] K.W. Lee, MS thesis, Tamknag University, Taiwan, ROC, 1997
- [18] R. Hoffmann, Solids and Surfaces: A Chemist's View of Bonding in Extended Structure, VCH, New York, 1988.
- [19] R.G. Parr, W. Yang, Density-functional Theory of Atoms and Molecules, Oxford University Press, New York, 1989.
- [20] J. Ihm, Rep. Prog. Phys. 51 (1988) 105.
- [21] M.C. Payne, M.P. Teter, D.C. Allan, T.A. Arias, J.D. Joannopoulos, Rev. Mod. Phys. 64 (1992) 1045.
- [22] M.P. Teter, M.C. Payne, D.C. Allan, Phys. Rev. B 40 (1989) 12255.
- [23] J.P. Perdew, in: P. Zeische, H. Eschrig (Eds.), Electronic Structure of Solid '91, Akademie, Berlin, 1991.
- [24] J.D. Monkhorst, Pack, Phys. Rev. B 13 (1976) 5188.
- [25] L. Kleinman, D.M. Bylander, Phys. Rev. Lett. 48 (1982) 1425.
- [26] D.R. Hamann, M. Schluter, C. Chiang, Phys. Rev. Lett. 43 (1979) 1494.
- [27] G. Kerker, J. Phys. C 13 (1980) L189.
- [28] G.B. Bachelet, D.R. Hamann, M. Schluter, Phy. Rev. B 26 (1982) 4199.
- [29] G.P. Kerker, J. Phys. C 13 (1980) L189.
- [30] A.M. Rappe, K.M. Rabe, E. Kaxiras, J.D. Joannopoulos, Phys. Rev. B 41 (1990) 1227.
- [31] J.S. Lin, A. Qteish, M.C. Payne, V. Heine, Phys. Rev. B 47 (1993) 4174.
- [32] J.S. Lin, M.C. Payne, V. Heine, J.D.C. McConnell, Phys. Chem. Minerals 21 (1994) 150.
- [33] I. Stich, M.C. Payne, R.D. King-Smith, J.S. Lin, L.J. Clarke, Phys. Rev. Lett. 68 (1992) 1351.
- [34] A. De Vita, M.J. Gillan, J.S. Lin, M.C. Payne, I. Stich, L.J. Clarke, Phys. Rev. Lett. 68 (1992) 3319.
- [35] V. Milman, S.J. Pennycook, D.E. Jesson, Thin Solid Films 272 (1996) 375.
- [36] J. Dabrowski, M. Scheffler, Appl. Surf. Sci. 56-58 (1992) 15.
- [37] J.S. Lin, Y.T. Kuo, M.H. Lee, K.H. Lee, J.C. Chen, submitted for publication.
- [38] R. Walsh, Acc. Chem. Res. 14 (1981) 246.
- [39] CASTEP, 3.5 ed., Molecular Simulations Inc., 1997.